Sumit Manohar Yadav* and Kamal Bin Yusoh

Sub-surface mechanical properties and sub-surface creep behavior of wood-plastic composites reinforced by organoclay

Abstract: Wood-plastic composites (WPC) were manufactured from polypropylene, wood flour, maleic anhydride grafted polypropylene and organoclay. The sub-surface mechanical properties and the sub-surface creep behavior of the organoclay-based WPC were examined by the nanoindentation technique. The results showed that the hardness, elastic modulus and creep resistance of the WPC enhanced with the loading of C20 organoclay. This enhancement was subject to the organoclay content and the dispersion of organoclay in the polymer matrix. The hardness, elastic modulus and creep resistance of WPC with 1 wt% organoclay content enhanced by approximately 36%, 41% and 17%, respectively, in contrast with WPC without organoclay. To study the impact of organoclay content on the creep performance of WPC, a viscoelastic model was actualized. The results demonstrated that the model was in good agreement with the experimental information. Reinforcement of organoclay prompts expansion in elastic deformation and instigates a higher initial displacement at the early stage of creep.

Keywords: nanoindentation; organoclay; sub-surface creep behavior; sub-surface mechanical properties; wood-plastic composite.

1 Introduction

Wood has numerous advantages as an engineering material, for example, its applications in construction, decking, fencing and furnishing. Nonetheless, wood, like other natural products, can be degraded by fungus and assaulted by termites. Moreover, the dimensional stability of wood is strongly influenced by the relative humidity in the environment. Due to these disadvantages, wood should be occasionally treated with some hazardous chemicals to prevent degradation. Chromated copper arsenate (CCA) has been widely applied to reduce the degradation of natural timber. However, the Environmental Protection Agency (EPA) phased out the CCA-treated wood from the building products market at the end of December 2004 [1]. This law, importantly, promotes the development of alternative materials such as wood-plastic composites (WPC).

The term wood plastic composites generally means compounding of wood flour (WF) with thermoplastic polymers such as polystyrene, polyethylene, polypropylene (PP), polyvinyl chloride or acrylonitrile-butadienestyrene. However, the wood loading in the polymer matrix is high; the smell and appearance of WPC are similar to natural timber (wood).

WPC exhibit the best properties of the neat components and thereby exhibit outstanding performance. Moreover, WPC have the advantage of good dimensional stability (i.e. lower water uptake and better durability against insects and fungi compared with wood) during their lifetime [2]. They are thus used in construction engineering such as decking for terrace and balconies.

Nowadays, for the amendment of WPC properties, nanofillers are being consistently used as great potential filler materials [3]. The term nanometer is used to define nanometer scale items (10^{-9} m). A nanometer is equal to billionth of a meter and nanofillers are smaller than the wavelength of visible light [4]. The application of nanofillers in the field of composites has set up new patterns of prospect to overwhelm the limitations of conventional micrometer scale fillers, since the nano-scale fillers are free from defects [5]. The surface area of nanofillers is larger than that of micro-scale fillers. Nanocomposites show more interphase region than micro composites [6]. Nanofillers demonstrate better reinforcement for the production of composites because they have a high aspect ratio (proportion of the largest to smallest dimension) [7].

To improve modulus, tensile properties, flame resistance, thermal stability and barrier properties, nanoclay is presently being applied as a nanofiller into the composite.

*Corresponding author: Sumit Manohar Yadav, Department of Wood and Paper Sciences, Kyungpook National University, Daegu 41566, Republic of Korea, e-mail: sumitmyadav13@gmail.com
Kamal Bin Yusoh: Faculty of Chemical Engineering and Natural Resources Engineering, Universiti Malaysia Pahang, 23600 Kuantan, Pahang, Malaysia

Due to its eco-friendliness, easy availability, low cost and well-understood chemistry, nanoclay is widely used as reinforcement for the polymer-clay nanocomposite [8]. One of the main advantages of using nanoclay particles in a polymer matrix is the substantial increase in the mechanical properties with the loading of less amount of nanofiller (<10 wt%) [9].

However, due to their nano dimensions which are normally in the range of nanometer dimensions and size, nanofillers forced a huge challenge for experimental equipment to describe their functions in WPC. However, significant improvement in WPC incorporated by nano-fillers has been made, but their dispersion mechanism and load transfer are still not thoroughly understood. It is a very long way from conclusions. The tensile test has widely been applied to study the mechanical proper-ties and elastic/plastic deformation of nanofiller-based polymer composites, with respect to the conventional mechanical testing. Because of the load and displacement resolution restrictions of the microscopic tensile tester, the observations of the stress behavior at the nanoscale level are relatively impossible [10]. The preparation of a tensile test specimen might create surface stress/strain concentration and surface flaws on the tensile specimen; due to this it becomes challenging to evaluate the defor-mation behavior and mechanical properties of composites at the nano level. To study the effect of nanofillers on the deformation behavior and mechanical properties of mate-rials, the nanoindentation technique is the most reliable, accurate and advance technique [11].

Several studies have been performed on the defor-mation behavior and mechanical properties of polymer nanocomposites [12]. However, the viscoelastic behavior of nanocomposites such as stress relaxation and creep is still not completely investigated. With regard to the nature of polymeric materials, it is viscoelastic materials whose properties are inadequate with the time. For instance, creep of a material is subjected to a stress beneath its yield stress and it is a time-dependent plastic deformation of a material. The mobility of polymer chains is completely responsible for the deformation process of a material under load. The chain mobility of polymer is subject to the temperature and time. The use of polymer and polymer-based materials can be affected by the time-dependent creep deformation [13].

To the best of our knowledge, very few studies have been performed on the measurement of the sub-surface mechanical properties and sub-surface creep behavior of fiber-reinforced polymer composites by using the nanoin-dentation technique. This new approach has not been applied to evaluate the sub-surface mechanical properties

and sub-surface creep behavior of nanoclay-based WPC. In this article, the experimental and modeling approaches of the surface mechanical properties and sub-surface creep behavior of nanoclay-based WPC are presented.

2 Materials and methods

2.1 Materials

Polypropylene (G 112) was supplied by Polypropylene Malaysia Sdn Bhd (Malaysia), and WF was supplied by Leong Seng Sawmill (Gambang, Malaysia). Maleic anhy-dride grafted polypropylene (MAPP) was purchased from Chemtura (China), and organoclay (Cloisite 20A) from Southern Clay Products, Inc. (Gonzales, TX, USA).

2.2 Preparation of wood-plastic composite

Initially, according to the formulations given in Table 1, organoclay, WF, PP and MAPP were weighed. Before being used in the composite, all the fillers were dried at 85°C in a convection oven for 48 h. The mixtures were pre-pared by using a single screw extruder (Brabender GmbH & Co. KG, Germany). The heating temperature profile of the screw was set at 190°C in the feed zone, 180°C in melting, and the extruder die was held at 170°C. The screw speed was 80 revolutions per minute and the die size was 5 mm. Before being fed into the first zone of the extruder, the organoclay, WF, PP and MAPP were premixed. The extruder strand passed through a water bath and was subsequently palletized. Finally, six sets of composite and blend samples were fabricated.

The compounded pallets were dried at 80°C for 24 h before injection molding to remove the remaining mois-ture. To produce the dumbbell-shaped specimens (ASTM 638 IV), the pallets were injection molded in a BOY 22M machine. The processing temperatures were set at 190°C

Table 1: The composition of designed formulations.

Samples	Polypropylene (wt%)	Wood flour (wt%)	MAPP (wt%)	Organoclay (C20)
PP	100	0	0	0
WPC	78	20	2	0
WPC/C20-1	77	20	2	1
WPC/C20-2.5	75.5	20	2	2.5
WPC/C20-4	74	20	2	4
WPC/C20-5	73	20	2	5

in the feed zone, 180°C in the melting and 170°C in the die zone. The cooling time was 20 s, clamping pressure 160 bars, injection pressure 100 bars and plasticizing back pressure 5 bars. The injection speed and screw rotation speed were 142 and 1 mm/min, respectively. Finally, the dumbbell-shaped specimens were conditioned at a relative humidity of $50 \pm 5\%$ and a temperature of 23 ± 2°C for at least 40 h according to ASTM D618-99 [14]. Three types of samples that were obtained are neat PP, WPC without organoclay and WPC reinforced by organoclay.

2.3 Characterization of wood-plastic composite

2.3.1 Transmission electron microscopy

Transmission electron microscopy (TEM) analysis was employed with scale bar 100 nm to study the distribution of nanoclay inside the composites. WPC sample powder was used for TEM analysis. Initially, composite powder was mixed with water and then dropped on 400 mesh copper grids. The analysis was conducted using a ZEISS LIBRA 120 instrument with 120 kV accelerating voltage.

2.3.2 Nanoindentation analysis

In this study, a completely calibrated Nano Test (Micro Materials, Wrexham, UK) was used to perform the interfacial sub-surface mechanical properties and sub-surface creep behavior of PP and organoclay-based WPC. A three-sided pyramidal-based Berkovich diamond indenter tip was used in this test. Using a suitable adhesive, a $1\,\text{cm} \times 1\,\text{cm} \times 1000\,\mu\text{m}$ catted specimen was mounted onto the nanoindentation sample stub and all tests were performed at room temperature. The experimental indentation parameters were the same for all measurements. The typical parameters are as follows:

- Initial load: 0.10 mN
- Maximum load for all indents: 10 mN
- Loading and unloading rate (strain rate): 0.50 mN/s

Since the polymer is a time-dependent material, to control the load applied on the composite samples, the constant strain rate was used. At the maximum depth, in order to measure creep effects, the indenter was held for 180 s at peak load before unloading. The distance between two indentation points was 30 μm, to avoid the overlapping problem. Average values were obtained from the measurements of 10 indentations (two indentations per sample of same composition).

The hardness (H) and elastic modulus (E) of composite samples can be determined by applying the Oliver and Pharr method with the help of load displacement information or data [11]. The plastic and elastic deformation occurs when the indenter enters into the composite sample. However, unloading recovers only the elastic portion of the displacement. Nanoindentation hardness is derived as follows:

$$H = \frac{P_{\max}}{A}, \tag{1}$$

where $P_{\max}$ is the load measured at peak depth of penetration (h) in an indentation; A is the projected area. $A = 24.5\,h^2$, an ideal Berkovich indenter [15].

The unloading curve information can be used to derive the reduced modulus of the sample. A relationship is expressed in the following equation:

$$E_{r} = \frac{\sqrt{\pi}}{2} \frac{S_{\max}}{\sqrt{2}}, \tag{2}$$

where E_{r} is the decreased elastic modulus and $S_{\max}$ represents the slope of the unloading curve at the point of maximum load.

The following equation shows the relationship between reduced modulus, E_{r}, and elastic modulus, E_{s} [11]:

$$\frac{1}{E_{r}} = \frac{(1-V_{s})^2}{E_{s}} + \frac{(1-V_{i})^2}{E_{i}} \tag{3}$$

where E and V with subscripts "s" and "i" are the elastic modulus and Poisson's ratio of the material and the indenter, respectively.

3 Results and discussion

3.1 Transmission electron microscopy

Scanning electron microscopy (SEM) analysis can be applied to understand the distribution of nanoclay particles in the polymer matrix; however, it may only give a brief suggestion on the degree of intercalation of the nanoclay layers due to the comparatively low-resolution capacity of SEM. TEM has a more intensive and monochromatic electron beam that creates a lesser cross-over diameter. This smaller cross-over in TEM, which is the point at which the electrons are focused when leaving the electron gun, gives a smaller final electron spot, thus creating higher resolution. In this study, TEM was conducted
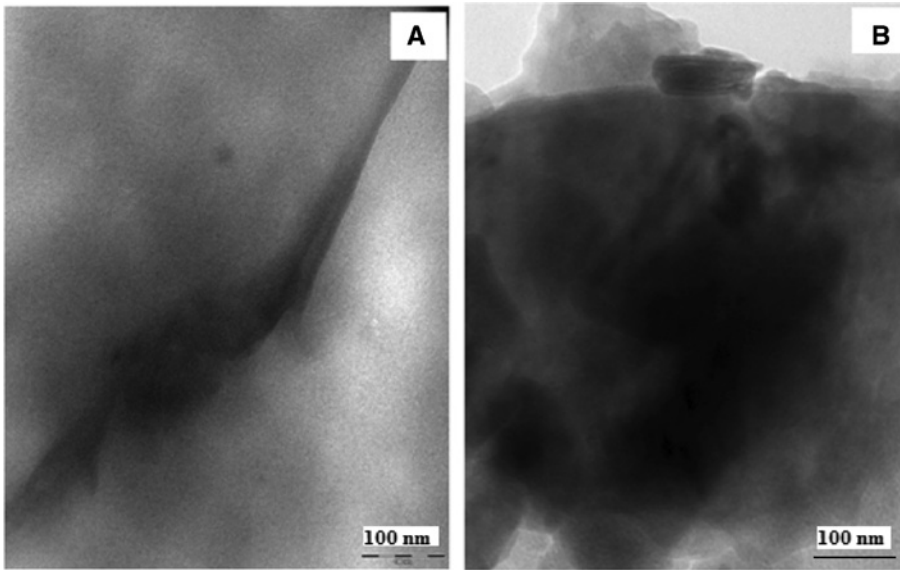
Figure 1: TEM micrographs of WPC with (A) 1 wt% C20 and (B) 5 wt% C20 (100 nm scale).

to observe a more detailed structure of nanoclay particle distribution in the composite.

Figure 1A and B show the TEM micrograph of WPC with 1 and 5 wt% C20 organoclay, and the nanocomposites were magnified to 100 nm in order to obtain a clearer and in-depth picture of the nanoclay particles and aggregates. In these micrographs, filamentary dark lines are related to intersection of silicate layers and the light regions correspond to the polymer matrix. As can be seen from Figure 1A, the C20 organoclay showed better dispersion and intercalation of nanoclay with PP in the WPC when 1 wt% of C20 organoclay was loaded into the composite. However, as can be seen in Figure 1B, with the increase in level of C20 organoclay loading to 5 wt%, the size of nanoclay particles became larger or aggregated and reduced the degree of intercalation. In other words, at higher loading, organoclay agglomeration occurs and the applied load will be distributed unevenly between non-agglomerated and agglomerated organoclay. It will affect the mechanical properties of the composite. Zhao et al. [16] reported similar examination while investigating the mechanical properties of the WF/polyvinyl chloride matrix/organoclay composite.

3.2 Sub-surface mechanical properties

In sub-surface indentation of a material, an indenter penetrates into the material with loaded force. A time of single loading and unloading cycle curve can be used to record the data. The information with respect to the plastic, viscoelastic and elastic behavior of a material can be obtained from the sub-surface indentation test [17].

Figure 2 depicts the loading and unloading indentation curve of PP, WPC and WPC loaded with different concentrations of C20 organoclay. It can be seen in the figure that the every composite sample shows a different mechanical response. The loading curves are followed by a period of holding time of 180 s at which the peak loads are 10 mN. The indentation curves of samples are shifted on left with the addition of C20 organoclay into the composite. It means that the WPC resistance to indentation significantly increases with the addition of organoclay. For the PP and WPC, the indenter reached at the maximum depth of 2129 and 1913 nm, respectively. The maximum depth of WPC reached at 1595 nm, when 1 wt% of organoclay had been introduced into the composite.
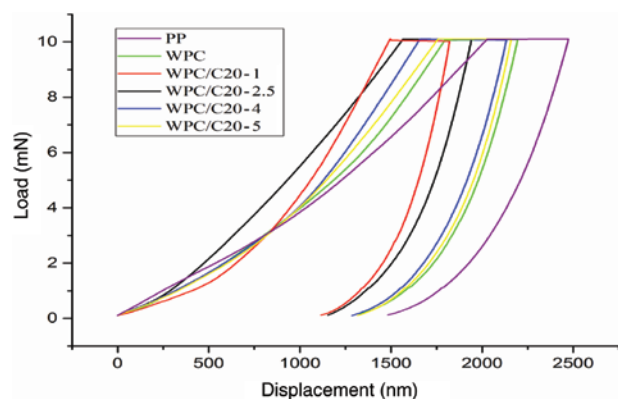
Figure 2: Typical indentation load-displacement curves for PP, WPC and WPC with different C20 organoclay concentrations.

The indentation depth represents the contributions from both plastic and elastic displacements.

The unloading curve discontinuity of the neat PP, WPC and WPC filled with nanoclay noticed at around 0.50 mN exhibits a recovery in the composite surface. The incorporation of organoclay into the WPC results in the yield strength of the WPC being increased, as per results obtained by the nanoindentation test.

The resistance of a material to the local deformation represents the hardness value (H) of the composite, whereas the overall stiffness of the composite represents the elastic modulus (E). The obtained nanoindentation test data were used to compute the reduced modulus and hardness values of the composite. Equation (2) was then used to calculate the elastic modulus of the composite. Figure 2 shows the hardness and modulus plot of PP, WPC and WPC with different C20 organoclay concentration. The hardness and modulus of the composite were increased over PP when WF was incorporated into the PP, as shown in Table 2. The reason might be the high degree of hardness and stiffness introduced by the incorporation of WF in the composite [18].

It can be seen from Table 2 that the loading of C20 organoclay into the composite increased both the hardness and the elastic modulus of WPC. With loading of 1 wt% content C20 organoclay, the hardness and modulus increased nearly 36% and 41%, respectively. However, with the high loading, the nanoclay created a poor dispersion in WPC due to agglomeration of nanoparticles and then the hardness and elastic modulus started to reduce, so the composite with 5 wt% nanoclay revealed the minimum hardness and elastic modulus. The same pattern was observed by Shen et al. in epoxy/organoclay nanocomposites, the sub-surface mechanical properties exhibiting littler increments above 2.5 wt% nanoclay content because of the agglomeration of nanoclay particles [19]. It can be concluded that dispersion of the nanoclay nanoplatelets in the polymer matrix is one of the most important factors controlling the elastic modulus and hardness in polymer nanocomposites.

Table 2: Hardness and modulus values of PP, WPC and WPC with C20 nanoclay loading.

Sample	Hardness (GPa)	Modulus (GPa)
PP	0.089±0.003	1.774±0.04
WPC	0.1105±0.004	2.402±0.04
WPC/C20-1	0.1581±0.003	3.410±0.03
WPC/C20-2.5	0.1437±0.003	2.887±0.03
WPC/C20-4	0.1182±0.002	2.501±0.03
WPC/C20-5	0.1141±0.004	2.475±0.04

3.3 Sub-surface creep behavior

Figure 3 depicts the creep displacement results of neat PP, WPC and WPC with different C20 organoclay concentrations. It is observed that the creep deformation decreased with the addition of nanoclay into a composite. WPC reinforced with organoclay show lower creep deformation over neat PP and WPC at the same load after 180 s. After 180 s of creep time, the creep displacements of 1, 2.5, 4 and 5 wt% of organoclay-reinforced composites were decreased to 292, 242, 69 and 38 nm, respectively, over the WPC. In general, a decline in creep displacement and rate has been observed in polymer nanocomposites with the addition of organoclay, demonstrating that the incorporation of rigid nanoclay nanofillers enhances the creep resistance [20–22]. A better interaction of polymer matrix and organoclay can contribute to an increase in the creep resistance and it is more noticeable with just 1 and 2.5 wt% of organoclay content. The increment of creep displacement with 4 and 5 wt% of nanoclay content might be attributed to the nanoclay agglomerate formation into the composite.

This result is similar to that of polyurethane-reinforced organoclay nanocomposites whereby after a high loading of organoclay, the improving impact of organoclay was consistently reduced. The high concentration of organoclay could change the morphology or microstructure of the polymer matrix, which could have an adverse effect on the creep behavior of composites [19].

A generalized elastic-viscoelastic (EVE) model which is the refined form of the elastic-viscoelastic-viscous model [23] was used to model the obtained results of the creep test. The EVE model was applied to obtain a deeper insight into the creep response of the C20 organoclay
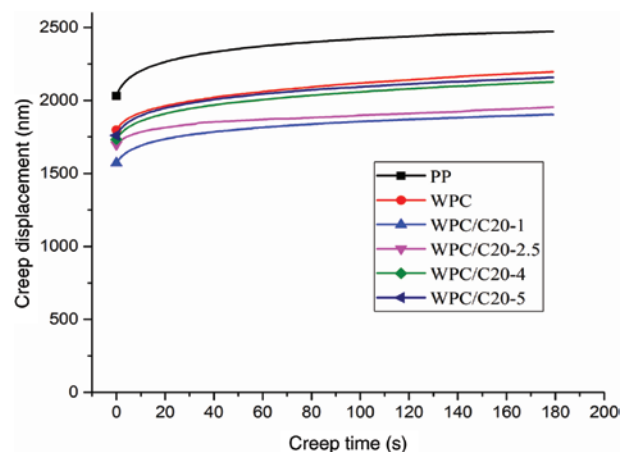
Figure 3: Creep displacement rate versus creep time for PP, WPC and WPC/C20 with different organoclay concentrations.

addition to the WPC. This model is a combination of a series of spring and dashpot which define the total displacement during the indentation creep test. Yang et al. [24] described this model in detail. According to this model, during the indentation, the creep deformation can be expressed as follows:

$$h = h_{in} \frac{P_o}{E_o A_o} + \sum_{i}^{n} \frac{P_o h_{in}}{E_i A_o} (1 - e^{-E_i\,t/n_i}) = h_e + \sum_{i}^{n} h_i (1 - e^{-t/\tau_i}) \quad (4)$$

where the indentation creep displacement is represented by h. h_{in} stands for the virtual length, which is used to express the indentation strain as in $\varepsilon = h/h_{in}$ and its value is equal to the elastic-plastic displacement. P_o and E_o represent the persistence indentation load for the indentation creep test and the elastic modulus of material, respectively. At the beginning of the indentation creep test, the initial contact area is presented by A_o. The calibrated indenter area function can be used to express A_o.
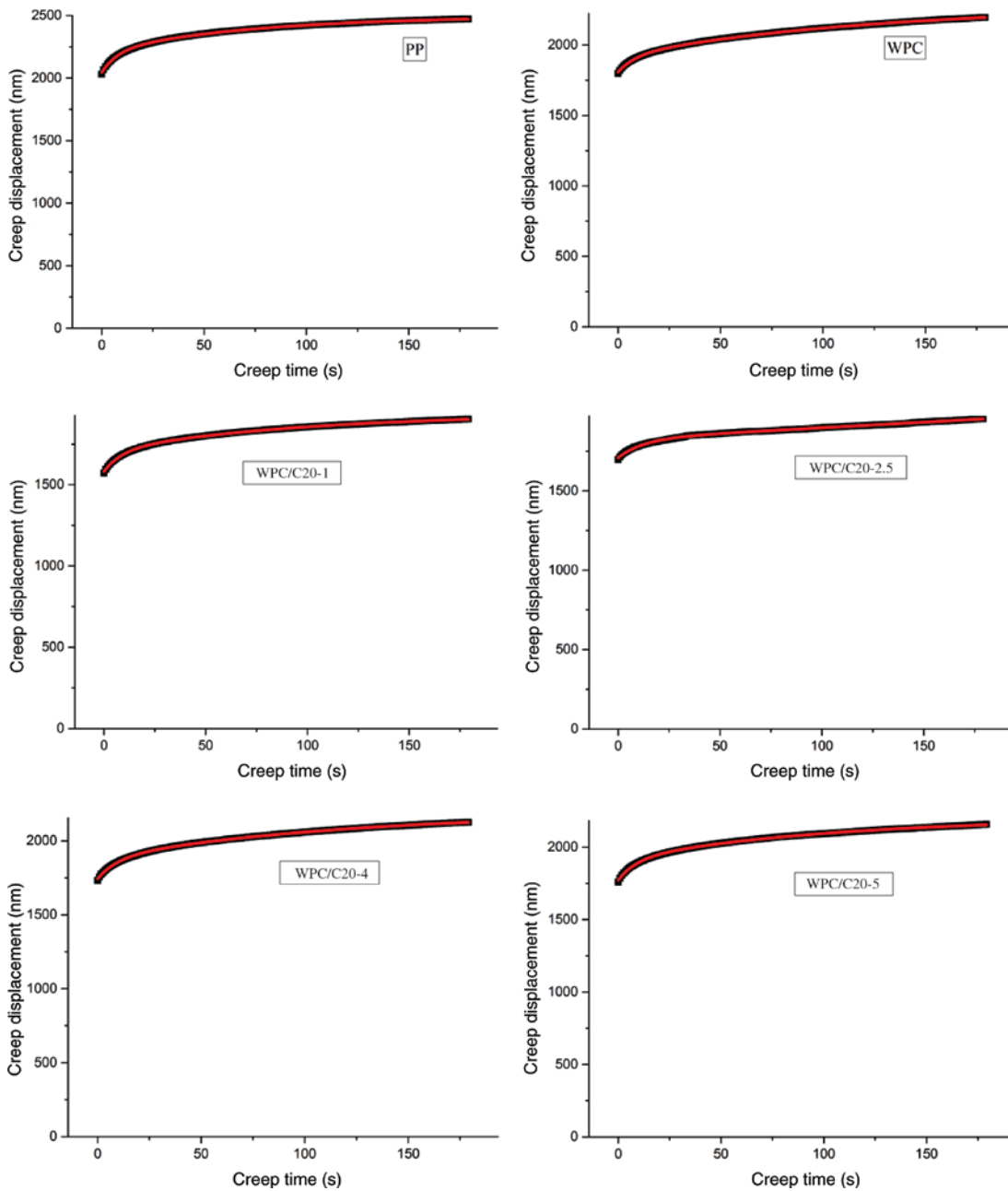
Figure 4: Creep versus time for PP, WPC and WPC/C20 with different nanoclay concentrations. The solid black line is experimental data and the thin red line is fitting results by Equation (4).

For the ith Kelvin unit in the model E_i is the elastic modulus and η_i is the viscosity coefficient. In the equation, n stands for the number of Kelvin units, with the value of n = 2, whereas t is the creep time [23]. The viscoelastic deformation controlled by the exponential terms during creep, according to the equation, and the deformation which is instantaneous displacement resulting from the elastic deformation of the materials during loading are the two contributions to the deformation which should be included in an indentation creep test.

This model can be applicable to the indentation creep data for the PP, WPC and nanoclay-based WPC. A satisfactory agreement of the model with the indentation creep data of PP, WPC and WPC with different concentrations of C20 organoclay is depicted in Figures 3 and 4.

Table 3 describes the fitting results based on Equation (4) for the indentation creep test of PP, WPC and WPC with different content of C20 nanoclay using a Berkovich indenter tip. According to the result, the value of instantaneous displacement, h_e, which is obtained by the elastic deformation, illustrates some decrement during loading of WF into the neat PP. The hardness and stiffness of WF possibly retard the initial process of creep, whereas the incorporation of nanoclay into a composite significantly decreases the initial creep process. At the initial stage, due to elastic deformation, the retardation of the creep process is improved by the loading of nanoclay into the composite. Nevertheless, the higher loading of nanoclay to 4 and 5 wt% of content induced a higher initial displacement at the early stage of creep and increased the elastic deformation. Possibly some changes in the structure of the polymer chains and the agglomeration of nanoclay in the polymer matrix might increase h_e. According to the above observation, it can be concluded that nanoclay dispersion into the composite has a significant role in controlling the creep in initial stages.

For viscoelastic behavior which is represented by h_1 and h_2, the presence of nanoclay shows a dramatic improvement in the creep performance of the composite over neat PP and WPC. According to the result, the WPC without nanoclay have lower h_1 and h_2 values than neat PP, whereas the values of h_1 and h_2 in WPC with 1 wt% nanoclay show a lower viscoelastic deformation compared to neat PP and WPC. The retardation times τ_1 and τ_2 are the response times, indicating that the WPC have lower retardant time than neat PP. In contrast, the retardation time became longer, with increasing nanoclay content into the WPC, particularly in τ_1, as demonstrated in Table 3. A good polymer matrix and nanoclay interactions might increase the retardation time in the composite.

4 Conclusions

The sub-surface mechanical properties and sub-surface creep behavior of organoclay-reinforced WPC were examined by means of the nanoindentation technique. The study investigated the influence of C20 organoclay loading on the hardness, elastic modulus and creep resistance of PP, WPC and WPC with different content of organoclay. According to the results, the hardness, elastic modulus and creep resistance significantly enhanced with the addition of C20 organoclay. However, with a higher loading of organoclay, the sub-surface mechanical properties and sub-surface creep resistance of composites decreased, due to the aggregation of organoclay particles. The improvement of the sub-surface mechanical properties and creep resistance of WPC confirmed that organoclay has great reinforcement and the ideal effect of nanoclay was achieved at 1 wt%.

Table 3: Fitting parameters from Equation (4) for polypropylene, WPC and WPC/C20 from the indentation creep experiment.

Parameter	PP	WPC	WPC/C20			
			1 wt%	2.5 wt%	4 wt%	5 wt%
h_e (nm)	2045	1807	1580	1709	1743	1772
h_1 (nm)	467	455	126	118	291	315
τ_1 (s)	474	323	13	96	103	118
h_2 (nm)	283	144	230	234	235	240
τ_2 (s)	9.66	9.30	8.30	8.33	8.63	8.80

References

[1] Yeh S-K. Polypropylene-based wood-plastic composites reinforced with nanoclay, PhD dissertation, 2007.

[2] Arao Y, Nakamura S, Tomita Y, Takakuwa K, Umemura T, Tanaka T. *Polym. Degrad. Stab.* 2014, 100, 79–85.

[3] Njuguna J, Pielichowski K, Desai S. *Polymer Adv. Tech.* 2008, 19, 947–959.

[4] Kamel S. *Express Polym. Lett.* 2007, 1, 546–575.

[5] Azeredo HM. *Food Res. Int.* 2009, 42, 1240–1253.

[6] Schadler LS, Brinson LC, Sawyer WG. *JOM* 2007, 59, 53–60.

[7] Rajeswari B, Malarvizhi N, Deenadayalan E, Jaisankar SN. *Polym. Plast. Technol. Eng.* 2017, 56, 883–888.

[8] Tjong SC. *Carbon Nanotube Reinforced Composites: Metal and Ceramic Matrices*, Wiley-VCH Verlag GmbH & Co. KGaA: Weinheim, Germany, 2009.

[9] Chavooshi A, Madhoushi M, Navi M, Abareshi MY. *Constr. Build. Mater.* 2014, 52, 324–330.

[10] Dutta AK, Penumadu D, Files B. *J. Mater. Res.* 2004, 19, 158–164.

[11] Merle B, Maier-Kiener V, Pharr GM. *Acta Mater*. 2017, 134, 167–176.

[12] Jin J, Song M, Yao KJ, Chen L. *J. Appl. Polym. Sci.* 2006, 99, 3677–3683.

[13] Gorrasi G, Tortora M, Vittoria V, Pollet E, Alexandre M, Dubois P. *J. Polym. Sci. B. Polym. Phys.* 2004, 42, 1466–1475.

[14] American Society for Testing and Materials (ASTM), ASTM D618-99:2002 Annual Book of ASTM Standards, West Consho-hocken, PA, 2002.

[15] International Organisation for Standarisation, ISO 14577-1.2, 2001, pp. 1–27.

[16] Zhao Y, Wang K, Zhu F, Xue P, Jia M. *Polym. Degrad. Stabil.* 2006, 91, 2874–2883.

[17] Beake BD, Leggett GJ. *Polymer* 2002, 43, 319–327.

[18] Yeh SK, Kim KJ, Gupta RK. *J. Appl. Polym. Sci.* 2013, 127, 1047–1053.

[19] Shen L, Wang L, Liu T, He C. *Macromol. Mater. Eng.* 2006, 291, 358–1366.

[20] Jin J, Yusoh K, Zhang HX, Song M. *J. Nanosci. Nanotechnol*. 2016, 16, 2576–2581.

[21] Adewole JK, Al-Mubaiyedh UA, Ul-Hamid A, Al-Juhani AA, Hussein IA. *Can. J. Chem. Eng.* 2012, 90, 1066–1078.

[22] Palacio M, Bhushan B, Ferrell N, Hansford D. *Sens. Actuator A Phys.* 2007, 135, 637–650.

[23] Seltzer R, Mai YW, Frontini PM. *Compos. Part B Eng.* 2012, 43, 83–89.

[24] Yang S, Zhang YW, Zeng K. *J. Appl. Phys.* 2004, 95, 3655–3666.